DMD Fast Forward. Published on July 30, 2007 as doi:10.1124/dmd.107.015800

Functional Induction of P-glycoprotein in the Blood Brain Barrier of Streptozotocin-induced Diabetic Rats: Evidence for the Involvement of NF-κB, a Nitrosative Stress-sensitive Transcription Factor, in the Regulation

HAN-JOO MAENG, MI-HWA KIM, HYO-EON JIN, SANG MI SHIN, TAKASI TSURUO, SANG GEON KIM, DAE-DUK KIM, CHANG-KOO SHIM, AND SUK-JAE CHUNG*

Department of Pharmaceutics, College of Pharmacy, Seoul National University, Seoul, Korea (H.-J.M., M.-H.K., H.-E.J., D.-D.K., C.-K.S., S.-J.C.); and National Research Laboratory, College of Pharmacy and Research Institute of Pharmaceutical Sciences, Seoul National University, Seoul, Korea (S.M.S., S.G.K.); and Graduate School of Pharmaceutical Science, The University of Tokyo, Tokyo, Japan (T.T.)

DMD Fast Forward. Published on July 30, 2007 as DOI: 10.1124/dmd.107.015800
This article has not been copyedited and formatted. The final version may differ from this version.

Running title: Functional induction of P-gp in STZ-induced diabetic rats

Address correspondence to:
Suk-Jae Chung, Ph.D.
Department of Pharmaceutics,
College of Pharmacy
Seoul National University
San 56-1 Shinlim-dong
Kwanak-gu
Seoul 151-742
Korea
Tel: +82-2-884-3170
Fax: + 82-2-885-8317
e-mail: sukjae@plaza.snu.ac.kr

Number of words	
Abstract	241 words
Introduction	654 words
Discussion	1464 words

Total number of text pages	34
Total number of figures	8
Total number of tables	3
Total number of references	40

List of nonstandard abbreviations used:

STZ, Streptozotocin; NO_x, nitrogen oxide(s); SNP, sodium nitroprusside; SIN-1, 3-morpholinosydnonimine; SNAP, S-nitroso-N-acetyl-DL-penicillamine; DETA, diethylenetriamine; HBSS, Hank's balanced salt solution; HEPES, 4-(2-hydroxyethyl)-1-piperazineethane sulfonic acid; MBEC4, mouse brain capillary endothelial cells; BBB, blood-brain barrier; RT-PCR, reverse transcription polymerase chain reaction; MDR, multidrug resistance; MRP, multidrug resistance protein; ABC, ATP binding cassette; NF-κB, nuclear factor-κB; iNOS, inducible nitric oxide synthase; SP-1, specific protein-1; EMSA, electrophoretic mobility shift assay

DMD Fast Forward. Published on July 30, 2007 as DOI: 10.1124/dmd.107.015800
This article has not been copyedited and formatted. The final version may differ from this version.

Abstract

The objective of this study was to investigate the transport kinetics of cyclosporin A, a well-known substrate for P-glycoprotein, across the blood-brain barrier (BBB), and the expression for the transporter in the brain of streptozotocin (STZ)-induced diabetic rats. The *in vivo* transport clearance of cyclosporine A was significantly reduced in diabetic rats compared with that in the control. The decreased transport was associated with the increased level of mRNA and the protein for P-glycoprotein in the rat brain. The functional activity of the efflux transporter in MBEC4 cells, an *in vitro* model of the BBB, was also stimulated when slow NO-releasing donors were present, whereas the stimulation was absent for the case of rapid NO-releasing donors (e.g., SNAP and DETA). The stimulatory effect was highest for SNP and the functional induction associated with the increased mRNA and protein level for the transporter. The pretreatment of the cell with SNP along with ascorbate, methylene blue or superoxide dismutase attenuated the induction of function and expression for P-glycoprotein, suggesting that the reaction product between superoxide and NO is involved in the induction of function and expression. The level of nuclear translocation of NF-κB and DNA binding activity of nuclear extracts to the NF-κB consensus oligonucleotide was increased in MBEC4 cells pretreated with SNP. Taken together, these observations suggest that nitrosative stress leads to the up-regulation of the message for the efflux transporter and, ultimately, to the enhanced

DMD Fast Forward. Published on July 30, 2007 as DOI: 10.1124/dmd.107.015800
This article has not been copyedited and formatted. The final version may differ from this version.

function, probably via a NF-κB-dependent mechanism.

DMD Fast Forward. Published on July 30, 2007 as DOI: 10.1124/dmd.107.015800
This article has not been copyedited and formatted. The final version may differ from this version.

Diabetes mellitus, an endocrine metabolic disorder, represents one of the most common geriatric diseases in developed countries (Rodriguez et al., 1996). Although the pathogenesis of the diabetes is not fully delineated, the literature information is quite clear on the involvement of oxidative and nitrosative stresses (Pacher et al., 2005; Cai et al., 2005) in the disease state. Nitrosative stress was defined as nitration/nitrosylation of protein, peroxidation of lipid, deoxyribonucleic acid (DNA) damage, and cell death caused by an excessive production of peroxynitrite and/or other reactive nitrogen species [viz, collectively nitrogen oxides (NO_x)] (Obrosova et al., 2004). These stress conditions may be associated with the development of diabetic complications such as cardiovascular disease, nephropathy and retinopathy (Krolewski et al., 1987). While it is possible that these stress conditions are independently related to the complications, the mediators for these stress conditions may also be involved cooperatively in the pathogenesis of the diabetes. For example, superoxide anion is known to react chemically with NO to form peroxynitrite, a highly reactive nitrogen oxide form (Huie and Padmaja, 1993), thereby potentially exacerbating the condition. Indeed, Cai and co-workers (2005) reported a significant increase of 3-nitrotyrosine, a by-product of the reaction between peroxynitrite and proteins, in the serum and tissue of a streptozotocin (STZ)-induced diabetic model, which may lead to an alteration in the function of the covalently modified proteins and, ultimately, of the organ itself. Despite the aforementioned possibility, however, the pathological impact of the

nitrosative stress was not fully delineated in the diabetes, especially for the case of the relationship between the stress conditions and pharmacokinetic alteration during the disease state.

It is becoming increasingly clear that NO_x is crucial regulatory mediators for the function and the expression of the transporter (Uchiyama et al., 2005). For example, Bridge et al. (2001) have shown that taurine transporter was up-regulated after long-term exposure to NO_x donors with cultured ARPE-19 cells. In addition, Uchiyama et al. (2005) reported that sodium-dependent neutral amino acid transporter was induced by the pretreatment of a NO_x donor with Caco-2 cells. Since the exposure with NO_x led to a regulation of more than one transport system in a number of different cell lines, a similar consequence may occur for pathological conditions that are associated with nitrosative stress, such as diabetes. Consistent with this hypothesis, the level of expression for ATP-binding cassette (ABC) transporters [e.g., MDR2/P-glycoprotein, (Van Waarde et al., 2002)] was increased in the liver of rats with experimental diabetes. Interestingly, Liu and coworkers (2006) showed the functional impairment of P-glycoprotein in the blood brain barrier of rats with experimental diabetes. Since the former literature indicates the existence of functional induction for ABC-transporters, including MDR2/P-glycoprotein in the liver of diabetic rats, a regulatory mechanism specific for the blood brain barrier may exist in the case of P-glycoprotein in diabetic conditions. Unfortunately, however, this aspect of P-

DMD Fast Forward. Published on July 30, 2007 as DOI: 10.1124/dmd.107.015800
This article has not been copyedited and formatted. The final version may differ from this version.

glycoprotein regulation has not been extensively studied in the brain of diabetic rats.

The current study, therefore, was undertaken to investigate the underlying mechanism for the functional alteration of P-glycoprotein in the blood brain barrier (BBB) of the STZ-induced diabetic rats and an *in vitro* model of the BBB [viz, MBEC4 cells (Tatsuta et al., 1992; Ahn et al., 2004)] pretreated with NO_x donors. Since diabetes is known to produce a nitrosative stress condition and the exposure of NO_x may lead to a regulation of the gene expression of efflux transporters (Heemskerk et al., 2007), the role of NO_x in the functional alteration of P-glycoprotein in the BBB was of particular interest. But rather than an impairment, it was found that an STZ-induced diabetic condition led to a functional induction of P-glycoprotein in the BBB in association with the increased levels of the protein and the corresponding mRNA of P-glycoprotein. The induction was apparently mediated by the activation of NF-κB, which is a putative regulatory factor for P-glycoprotein gene expression and a nuclear transcription factor that is sensitive to nitrosative stress.

DMD Fast Forward. Published on July 30, 2007 as DOI: 10.1124/dmd.107.015800
This article has not been copyedited and formatted. The final version may differ from this version.

MATERIALS AND METHODS

Materials

[^{3}H] cyclosporin A (CsA, specific activity 9 Ci/mmol) and [^{14}C] mannitol (specific activity 53.7 mCi/mmol) were purchased from Amersham Pharmacia (Piscataway, NJ). Streptozotocin (STZ), sodium nitroprusside (SNP), 3-morpholinosydnonimine (SIN-1), S-nitroso-N-acetyl-DL-penicillamine (SNAP), diethylenetriamine (DETA), methylene blue, ascorbate, superoxide dismutase (SOD), Dulbecco's modified Eagles' medium, nonessential amino acid solution, penicilline-streptomycin, Hank's balanced salt solution (HBSS) and HEPES were obtained from Sigma-Aldrich (St. Louis, MO). Fetal bovine serum and trypsin-EDTA were purchased from Gibco Laboratories (Gaithersburg. MD). MBEC4 cells were previously generated by our research group (Tatsuta et al., 1992). All other chemicals were of reagent grade or better, and were used without further purification.

Animals

Male Sprague-Dawley rats (Dae-Han Biolink, Eumsung, Korea), weighing 220~230 grams, were used in this study. Experimental protocols involving animals in this study were reviewed by the Animal Care and Use Committee of the College of Pharmacy, Seoul National University, according to National Institutes of Health guidelines (NIH publication number 85-23, revised 1985) *"Principles of Laboratory Animal Care"*

Induction of Experimental Diabetes in Rats by STZ Administration

The rats were randomly divided into two groups: control and diabetes. Freshly prepared STZ solution (i.e., STZ powder dissolved in a citrate buffer of pH 4.5, the final concentration for STZ of 60 mg/ml) at a dose of 60 mg/kg was administered once via intraperitoneal injection to overnight-fasted rats. Control rats received an intraperitoneal injection of the same volume of citrate buffer (i.e., the vehicle). On day 3, blood samples (50 µl, via tail vein blood sampling) were obtained from the rats for the determination of blood glucose level. The rats having a blood glucose level exceeding 300 mg/dl (determined by One Touch® (glucometer), LifeScan Inc., Milipitas, CA) were considered to be experimental diabetic and used in subsequent studies. All rats were maintained for up to 28 days with free access to food and tap water in temperature- and humidity-controlled quarters. Blood glucose concentrations and weights were monitored weekly and subsequent doses were provided as necessary.

Determination NO_x

NO_x level of plasma or NO_x donors under our cell culture conditions was measured spectrophometrically by the use of the Griess reaction (Green et al., 1982). Approximately 400 µl of blood samples were obtained from control or diabetic rats, and the plasma was obtained by centrifugation (14,000 rpm, for 15 min). Nitrate contained in the sample was first reduced by nitrate reductase to nitrite and the Griess reagent, a mixture (1:1) of 0.2% naphthyethylene-

diamine and 2% sulfonamide in 5% phosphoric acid, was then added. After 5 min standing at room temperature, the concentration of total nitrite was determined spectrophotometrically at 550 nm using $NaNO_3$ solution as the standard. Total nitrite level was regarded as the sample NO_x concentration.

***In Vivo* Brain Uptake Study**

Under light ether anesthesia, the rats received implantations in their femoral artery and vein, using catheters made of polyethylene tubing (PE-50; Clay Adams, Parsippany, NJ) filled with heparinized saline (25 U/ml). After recovery (i.e., approximately 120 min after the completion of the surgery) from anesthesia, CsA solution was bolus injected to the rat via the venous catheter at the dose of 1 mg/kg. Each dosing solution contained 1mg of CsA in 1 mL of the vehicle (PEG400 : ethanol = 9 : 1). The blood samples were collected at 30, 60, 120 and 180 sec. Immediately after the last blood collection, the rat was decapitated, the brain tissue collected and weighed. The blood and brain samples were then solubilized in 1 ml of Soluene-350 (Packard Bioscience, Groningen, Netherlands) and transferred to scintillation vials for the determination of radioactivity. The brain uptake clearance was estimated by standard integration plot analysis (Kusuhara et al., 1997), in which the uptake clearance was obtained by dividing the amount of CsA in the brain at time t by the area under the plasma concentration-time curve upto the time t for CsA.

Real-time PCR Analysis

When it was necessary to determine the mRNA levels for P-glycoprotein in the brain of control/diabetic rats and MBEC4 cells pretreated with SNP, real-time monitoring of the PCR reaction was performed using the LightCycler® 1.5 system (RocheApplied Science, Indianapolis, IN, USA). Pairs of forward/reverse primers specific for MDR1a, MDR1b, MRP1 MRP2 and β-actin were synthesized as described by Vliet et al. (2004) and Serrano et al. (2003). The FastStart DNA Master SYBR Green Kit (RocheApplied Science, Indianapolis, IN, USA) was used for the quantitative PCR analysis (Vliet et al., 2004). The cycling conditions were carried out as follows: MDR1a, MRP1 and MRP2: initial denaturation at 95˚C for 6 min, followed by 45 cycles of denaturation at 95˚C for 15 s, annealing at 59˚C for 5 s and extension at 72˚C for 10 s; MDR1b: initial denaturation at 95˚C for 6 min, followed by 45 cycles of denaturation at 95˚C for 15 s, annealing at 56˚C for 5 s and extension at 72˚C for 20 s. The temperature transition rate was set at $20^{\circ}Cs^{-1}$. To distinguish the specific amplification product from non-specific products or primer dimmers, a melting curve was constructed from the amplification reaction obtained by maintaining the temperature at 65˚C for 15 s, followed with a gradual temperature increase rate of 0.1˚C /sec to 95˚C. For this study, the signal acquisition mode was set at “continuous”.

The relative quantification of the amount of the target message in the tested brain

tissue samples was obtained by measuring C_t. The following equations were employed to quantify the amount of the message:

$$\Delta C_t = C_{t_{MDR1}} - C_{t_{\beta\text{-actin}}} \quad (1)$$

$$C_{t_{Linear}} = 2^{-(\Delta Ct,treated - \Delta Ct,control)} \quad (2)$$

where $C_{t_{MDR1}}$ represents the C_t value of the target gene and $C_{t_{\beta\text{-actin}}}$ the C_t value of the endogenous control reference gene. $C_{t_{Linear}}$ represents the fold change in the mRNA expression between the control and the treated groups, assuming a doubling of the target sequence with each PCR cycle.

MBEC4 Cell Culture

For this study, MBEC4 cells, immortalized mice brain capillary endothelial cells (Tatsuta et al., 1992), were used as an *in vitro* model of the BBB. Standard protocols were used for subculturing in a T-flask and seeding in 12-well culture plates (Ahn et al., 2004). Cells were maintained at 37˚C in Dulbecco's modified Eagles' medium (low glucose), 10% fetal bovine serum, 1% nonessential amino acid solution, 100 units/ml penicillin, and 0.1 mg/ml streptomycin in an atmosphere of 5 % CO_2 and 90 % relative humidity.

Determination of CsA Uptake in MBEC4 cells

When it was necessary to determine the uptake kinetics, the culture medium was removed from MBEC4 cells and the cells were subsequently washed three times with uptake

DMD Fast Forward. Published on July 30, 2007 as DOI: 10.1124/dmd.107.015800
This article has not been copyedited and formatted. The final version may differ from this version.

buffer. The uptake buffer contained HBSS with 25 mM HEPES and 25 mM glucose (pH 7.4). Uptake was initiated by addition of 1 ml of uptake buffer containing 1 μM CsA with trace levels (i.e., 1% of total CsA concentration) of the radiolabeled drug. Fifteen min uptake at 37˚C was measured for this study. Upon completion of the incubation, the uptake was terminated by the aspiration of medium followed by washing (three times) with ice-cold uptake buffer with unlabeled CsA. The cells were then solubilized in 1 ml of 0.1 N NaOH and transferred to scintillation vials for the determination of radioactivity. The amount of uptake of [^{3}H] CsA was adjusted to pmol per mg protein in each sample.

CsA Uptake in the Presence of Various NO_x Donors in MBEC4 Cells

To determine the uptake of CsA in MBEC4 cells in the presence of various NO_x donors, confluent cultures of MBEC4 cells were incubated at 37˚C with serum-free medium in either the absence or the presence (viz, 1 mM for all donors, final concentration) of NO_x donors, SNAP, DETA, SIN-1 or SNP, for 24 hrs. Upon the completion of the pretreatment, the pretreatment media was aspirated, the cells were washed three times with uptake buffer, and the uptake of CsA was determined, similar to the procedure described in the previous section. When it was necessary to study the temporal dependency of the effect of SNP, the cells were pretreated with the donor for various periods of exposure (from 0.5 to 24 hr) and the uptake determined in a similar manner. Since the impact of SNP may be mediated by a number of different NO_x, SNP

DMD Fast Forward. Published on July 30, 2007 as DOI: 10.1124/dmd.107.015800
This article has not been copyedited and formatted. The final version may differ from this version.

mediated stimulation on the efflux of CsA was studied in MBEC4 cells by the pretreatment of SNP in the presence (all in final concentration) of either ascorbate [10 mM, an antioxidant (Bridges et al., 2001)], methylene blue [1 mM, an NO scavenger (Bridges et al., 2001)], or SOD [750 unit/ml, superoxide scavenger (Uchiyama et al., 2005)]. The potential cytotoxic effects of the NO_x donors (1 mM) were also evaluated by protein (Lowry et al., 1951) and MTT assays.

Total RNA Isolation and cDNA Synthesis

Total RNA was isolated from the brain tissues and the MBEC4 cells using a Trizol reagent (Invitrogen, Carlsbad, CA, USA) according to the manufacture's instructions. The concentration and purity of the RNA was determined spectrophotometrically at 260/280 nm. Approximately 1 μg of total RNA was used in each 20 μl reaction mixture containing 5 mM $MgCl_2$, 1 mM dNTP, 5 U RNase inhibitor, 5 U AMV reverse transcriptase, and 0.125 μM oligo-dT-adaptor primer (Takara Shuzo Co., Ltd., Shiga, Japan). The reactions were carried out by incubating the mixture at 42˚C for 30 min, heating to 99˚C for 5 min and subsequent cooling to 4˚C.

Semi-quantitative RT-PCR Analysis

When it was necessary to determine the mRNA levels for P-glycoprotein in MBEC4 cells, RT-PCR was carried out using primer pairs specific for mice MDR1b [5'-TGCTTATGGATCCCAGAGTGAC-3' (sense) and 5'-TTGGTGAGGATCTCTCCGGCT-3'

(antisense)]. The primers specific for mice GAPDH were 5'-CTCATgACCACAgTCCATgC-3' (sense) and 5'-CACATTgggggTAggAACAC-3' (antisense). The fragments of specific genes were amplified through 30 cycles of 94˚C for 1 min, 55˚C for 2 min and 72˚C for 2 min and terminated by a final step of 72˚C for 15 min. The PCR products were separated by gel-electrophoresis using 1.5% (w/v) agarose, then inspected under UV light after ethidium bromide staining and photographed using a digital camera.

Preparation of Nuclear and Cytosolic Fractions

Nuclear extracts were prepared essentially according to Schreiber et al. (1990). Briefly, cells in dishes were washed with ice-cold PBS. Cells were then scraped and allowed to swell after addition of 100 µl lysis buffer containing 10 mM HEPES (pH 7.9), 0.5% Nonidet P-40, 10 mM KCl, 0.1 mM EDTA, 1 mM dithiothreitol, and 0.5 mM phenylmethylsulfonyl fluoride. Cell membranes were lyzed by vortexing the mixture; the lysate was then incubated for 10 min on ice and centrifuged at 7200 g for 5 min. The supernatant (i.e., containing cytosolic fraction) was stored at -70˚C until use. The pellet (i.e., containing crude nuclei) was re-suspended in 50 µl of a buffer containing 20 mM HEPES (pH 7.9), 400 mM NaCl, 1 mM EDTA, 1 mM dithiothreitol, and 1 mM phenylmethylsulfonyl fluoride, then it was incubated for 30 min on ice. The samples were subsequently centrifuged at 15,800g for 10 min to obtain the nuclear extract (i.e., the supernatant). The nuclear extracts were stored at -70˚C until use.

DMD Fast Forward. Published on July 30, 2007 as DOI: 10.1124/dmd.107.015800
This article has not been copyedited and formatted. The final version may differ from this version.

Western Blot Analysis

Western blot analysis was performed to determine levels of P-glycoprotein of brain homogenate in rats or the lysates of MBEC4 cells pretreated with SNP. Western blot analysis was also performed to determine levels of NF-κB in the nuclear extract of MBEC4 cells exposed to SNP or by SNP exposure in the presence of ascorbate, methylene blue or SOD. The samples (20 μg for P-glycoprotein of brain homogenate in rats or NF-κB in the nuclear extract of MBEC4 cells or 100 μg for P-glycoprotein of the lysates of MBEC4 cells pretreated with SNP) were loaded on 10% polyacrylamide gel containing 0.1% sodium dodecyl sulfate and electrophoretic separation was carried out. The gel was then transferred onto a nitrocellulose membrane. The membrane was probed with either a primary monoclonal mouse antibody, C219 (Signet, Dedham, MA), for the determination of P-glycoprotein level, or with a rabbit polyclonal anti-NF-κB p65 (Santa Cruze Biotechnology, Santa Cruz, CA) for the determination of NF-κB level. Either peroxidase-conjugated anti-rabbit or anti-mouse immunoglobulin G (Zymed Laboratories, South San Francisco, CA) was used as a secondary antibody. The bound antibody was detected using an enhanced chemiluminescence detection system (Amersham Life Science, Buckinghamshire, UK).

Electrophoretic Mobility Shift Assay (EMSA)

A double-stranded DNA probe for the consensus sequence of nuclear factor-κB (NF-

DMD Fast Forward. Published on July 30, 2007 as DOI: 10.1124/dmd.107.015800
This article has not been copyedited and formatted. The final version may differ from this version.

κB, 5'-AGTTGAGGGGACTTTCCCAGGC-3') was used for gel shift analysis after end-labeling of the probe with [γ-^{32}P] ATP and T_4 polynucleotide kinase. The reaction mixture contained 2 μl of 5 X binding buffer with 20% glycerol, 5 mM $MgCl_2$, 250 mM NaCl, 2.5 mM EDTA, 2.5 mM dithiothreitol, 0.25 mg/ml poly (dI-dC), and 50 mM Tris·Cl (pH 7.5), 30 μg nuclear extracts, and sterile water in a total volume of 10 μl. Incubations were initiated by addition of 1 μl probe (10^6 cpm) and continued for 20 min at room temperature. The specificity of the DNA/protein binding was confirmed by competition reactions, in which a 20-fold molar excess of unlabeled NF-κB oligonucleotide was added to each reaction mixture before the addition of radiolabeled probe. For supershift assay, the antibody (2 μg) was added to the reaction mixture and additionally incubated for 1 hr at 25˚C. Samples were loaded onto 4% polyacrylamide gels at 100V. The gels were removed, fixed, and dried, followed by autoradiography.

Data Analysis

When it was necessary to determine the brain uptake clearance by integration plot method, the rate of the compound in the brain was calculated by equation 3 (Kusuhara et al., 1997).

$$X_{brain}(t) = CL_{uptake} \cdot AUC_0^t \quad (3)$$

where X_{brain} represents the amount of drug in the brain, CL_{uptake} represents the uptake clearance to the brain and AUC_0^t represents the area under the concentration time curve from time zero to

DMD Fast Forward. Published on July 30, 2007 as DOI: 10.1124/dmd.107.015800
This article has not been copyedited and formatted. The final version may differ from this version.

the time of brain sampling.

When it was necessary to compare the means between the treatments, the unpaired t-test or, one-way ANOVA, followed by Duncan's test, was typically used. For this study, $p < 0.05$ was accepted as denoting statistical significance. Data were expressed as the mean ± S.D..

DMD Fast Forward. Published on July 30, 2007 as DOI: 10.1124/dmd.107.015800
This article has not been copyedited and formatted. The final version may differ from this version.

RESULTS

Comparison of Body Weight, Blood Glucose Level and Plasma NO_x in Control vs. STZ-Administered Rats

For this study, blood glucose levels and body weights were monitored over the 28-day experimental period for both the control and the STZ-administered rats. After 28 days of administration, STZ-treated rats had a significantly lower body weight compared with control rats (Table 1). The body weight of the control rats increased continuously during the experimental period, while the body weight of the STZ-administered rats decreased during the same period. In addition, blood glucose concentration was significantly higher for the STZ-treated rats compared with the control rats (Table 1). The concentrations of blood glucose in the STZ-induced diabetic rats remained above 400 mg/dl (i.e., for 1-week, 403 ± 26.5 mg/dl; for 2-week, 450 ± 46.1 mg/dl; for 3-week, 494 ± 32.4 mg/dl; for 4-week, 500 ± 23.7 mg/dl), whereas blood glucose was significantly lower in the control rats (i.e., 71.5 ± 5.45 mg/dl). Table 1 shows that plasma NO_x concentrations were significantly elevated in STZ-induced hyperglycemic rats, compared with the control rats. Plasma NO_x concentrations in the STZ-induced diabetic rats were as follows: 70.6 ± 4.88 μM, 1-week; 120 ± 21.5 μM, 2-week; 124 ± 36.3 μM, 3-week; 117 ± 12.3 μM, 4-week.

The characteristics for STZ-induced hyperglycemic rats were consistent with those

found in the clinical diabetes (Szkudelski, 2001). In addition, the enhanced level of NO_x in the plasma was consistent with other experimental diabetic models (Bank et al., 1993). These observations suggest, therefore, that the STZ administration to the rats led to experimental diabetes in this study.

Kinetics of CsA Transport to the Brain in Control vs. STZ-induced Diabetic Rats

Since CsA is known to partition to red blood cells in a time-dependent manner, the blood concentration, rather than the plasma concentration was measured to determine the pharmacokinetics in this study. After an intravenous administration of CsA, a substrate of P-glycoprotein, at the dose of 1 mg/kg, the temporal profiles of mean arterial blood concentration for the immunosuppressive drug were not significantly different between control and STZ-induced diabetic rats, suggesting that the systemic pharmacokinetics was not affected by the diabetic condition (data not shown), consistent with the study of Ogata and co-workers (1996). In contrast, however, the transport of CsA to the brain was significantly different. Table 2 summarizes the kinetic parameters for CsA transport to the brain. While the brain-to-plasma concentration ratio for mannitol, a substance that is not permeable to the BBB (Ahn et al., 2004), was not affected (i.e., 40.6 ± 1.84 vs. 39.8 ± 1.21 µl/g brain for control vs. diabetic rats, respectively), the concentration ratio for CsA was significantly reduced in the diabetic rats (37.5 ± 7.43 µl/g brain), compared with the control rats (56.9 ± 5.66 µl/g brain). In addition, the

apparent brain uptake clearance by integration plot analysis (Kusuhara et al., 1997) was also reduced by the induction of diabetes (Table 2). When the brain uptake kinetics was monitored with the progression of the hyperglycemic condition (Fig. 1), the reduced penetration was readily apparent at 1-week after STZ administration, and the reduced penetration was continued throughout the experimental period (i.e., ~ 4-week).

Comparison of the Levels of mRNA and Protein for P-glycoprotein in Control vs. STZ-induced Diabetic Rats

Since the reduced penetration of CsA may be related to a functional induction of the efflux transporter (e.g., P-glycoprotein) for the drug, the levels of the mRNA and the protein for P-glycoprotein were examined in both the control and the STZ-induced diabetic rats. When mRNA levels of MDR1a and MDR1b were determined in brain homogenates by real-time RT-PCR, as indicated by the ΔC_t value, both were significantly increased compared to levels in the control rats ($p<0.001$) (i.e., for MDR1a, 4.01 ± 1.09 fold; for MDR1b, 2.91 ± 1.15 fold, Fig. 2). In addition, the MDR1a form was expressed higher than was the MDR1b form, the isoform of MDR1a, in the brain homogenate of the control rats, which is consistent with the literature (Mei et al., 2004). Similar to the change in MDR1 isoforms, the MRP2 mRNA expression was significantly increased in the brain of diabetic rats (2.28 fold of controls), whereas the MRP1 mRNA level was not affected by the induction of experimental diabetes (Fig.2).

When the protein level of the P-glycoprotein was determined by Western blot analysis using C219 antibody in the brain homogenates for both the control rats and the STZ-induced diabetic rats, the P-glycoprotein levels were markedly increased in the diabetic group, compared with the control (Fig. 3A). The density of the bands, as determined by an imaging software, indicated that P-glycoprotein expression was approximately 1.92 fold higher in the diabetic rats brain compared with the brain of the control rats (Fig. 3B). These results suggest that STZ-induced diabetes leads to an enhanced expression of mRNA and protein for P-glycoprotein in the brain. In addition, this observation was consistent with the reduced penetration of CsA in the *in vivo* kinetic study (Table 2 and Fig. 1).

Comparison of P-glycoprotein Functions in MBEC4 Cells in the Presence of NO_x Donors

In the literature, it was demonstrated that correlation of the efflux ratio (i.e., the function) for representative substrates between the mouse and the rat P-glycoprotein was statistically significant (i.e., correlation coefficient of 0.786 for MDR1a and correlation coefficient of 0.931 for MDR1b) (Takeuchi et al., 2006). In addition to the comparable functions between the rat and the mouse MDR1 protein, significant amino acid sequence homology was noted between the species (i.e., 94.7% between the rat and mouse form for MDR1a; 93% between the rat and mouse form for MDR1b). Based on the literature evidence, P-glycoproteins from the rat and mouse were regarded as functionally comparable in subsequent

DMD Fast Forward. Published on July 30, 2007 as DOI: 10.1124/dmd.107.015800
This article has not been copyedited and formatted. The final version may differ from this version.

studies. To study the underlying mechanism for the enhanced expression and the function of P-glycoprotein, MBEC4 cells, an *in vitro* model of the BBB (Ahn et al., 2004), was used. The level of NO_x generated from 1 mM NO_x donors in the cell culture condition is summarized in Table 3. The NO_x level (i.e., in order from the highest to the lowest) was DETA > SIN-1 > SNAP > SNP. The NO_x concentration in the plasma obtained from the diabetic rats was 117 ± 12.3 μM compared with a concentration of 158 ± 20.0 μM in incubation media that contained 1 mM SNP. Therefore, the level of NO_x exposure in the *in vitro* and *in vivo* experiments was relatively comparable. When the cell was exposed to NO_x donors, SNAP, DETA, SIN-1 or SNP, for 24 hr at the concentration of 1 mM, the functional alteration on the uptake of CsA in the MBEC4 cells was variable (Fig. 4). Amongst the NO_x donors, the functional enhancement (i.e., reduced uptake) was apparent for SNP and SIN-1, while the stimulatory effect was absent for SNAP and DETA. In the cases of the NO_x donors that exhibited the stimulatory effect, SNP was the most pronounced. Figure 4B shows the concentration-stimulation relationship for SNP in MBEC4 cells. The concentration dependent stimulatory effect was observed for the treatments at SNP concentrations higher than 100 μM. Temporal dependency of the stimulation by SNP showed that, after a transient impairment (i.e., 0.5~1 hr of the SNP treatment), the functional induction was readily apparent after 24-hr of the treatment (Fig. 4C). In subsequent studies, the treatment with SNP was set at 1mM/24 hr for the exposure time. To further test the functional

DMD Fast Forward. Published on July 30, 2007 as DOI: 10.1124/dmd.107.015800
This article has not been copyedited and formatted. The final version may differ from this version.

induction of P-glycoprotein in MBEC4 cells exposed to SNP, intracellular accumulation of CsA (initial concentration of 10 nM) in the presence and the absence of verapamil (10 μM, the final concentration in the transport media), a known inhibitor for P-glycoprotein function (Matsuzaki et al., 1999), was compared in control and SNP-pretreated MBEC4 cells. The accumulation of CsA was 3.51 ± 0.168 and 2.48 ± 0.147 pmol/mg protein in control and SNP-pretreated cells, respectively. Whereas, in the presence of verapamil (10 μM), there was greater accumulation of CsA, 4.94 ± 0.278 and 4.81 ± 0.684 pmol/mg protein in control and SNP-pretreated cells, respectively. This observation is consistent with the hypothesis that the functional induction by SNP-pretreated MBEC4 cells is mediated by the induction of P-glycoprotein. Collectively, these results indicate that SNP and SIN-1, but not all NO_x donors, had a stimulatory effect on the function of P-glycoprotein.

Comparison of the Levels of mRNA and Protein for P-glycoprotein in MBEC4 Cells with or without SNP Pretreatment

In a preliminary study, we attempted to measure the level of MDR1a in MBEC4 cells with quantitative RT-PCR. However, amplification curves for MDR1a could not be constructed up to 45 cycles with a number of annealing conditions, probably because of limited MDR1a expression in MBEC4 cells (Matsuzaki et al., 1999). Therefore, we measured only MDR1b in subsequent studies of MBEC4 cells. RT-PCR analysis was used to study the effect of SNP

DMD Fast Forward. Published on July 30, 2007 as DOI: 10.1124/dmd.107.015800
This article has not been copyedited and formatted. The final version may differ from this version.

treatment on the level of P-glycoprotein mRNA. The level of MDR1b mRNA was markedly increased in SNP-treated MBEC4 cells, compared with untreated cells (Fig. 5A). The level of a housekeeping gene, GAPDH, was not affected by the SNP treatment with MBEC4 cells (Fig. 5A). When mRNA levels of MDR1b were determined in SNP-pretreated MBEC4 cells by real-time RT-PCR, as indicated by the ΔC_t value, the level was significantly increased compared with untreated MBEC4 cells ($p<0.001$) (i.e., for MDR1b, 3.09 ± 0.28 fold, Fig. 5B). Consistent with the mRNA level, the level of P-glycoprotein protein was markedly increased approximately 1.74- fold in SNP-pretreated MBEC4 cells (Fig. 5C).

Potential Reversal of SNP-induced Stimulatory Effect on the Function and Expression of P-glycoprotein in MBEC4 Cells

Since not all NO_x donors had a stimulatory effect on the function of P-glycoprotein in MBEC4 cells, the possibility for reversal for the SNP-induced stimulatory effect was studied. An antioxidant, a NO scavenger, or SOD, was added to MBEC4 cells, along with a SNP treatment, and the functional activity / mRNA levels were examined (Fig. 6). The SNP-mediated stimulatory effect (i.e., reduced uptake) was partially reversed by the presence of ascorbate (i.e., an antioxidant, 10 mM) or methylene blue (i.e., an NO scavenger, 1mM) (Fig. 6A). The addition of SOD (i.e., 750 U/ml), a superoxide scavenger, also led to a partial reversal of the SNP-mediated stimulation on the function of P-glycoprotein (Fig. 6A). When mRNA levels of

MDR1b were determined in SNP-treated MBEC4 cells by real-time RT-PCR, as indicated by the ΔC_t value, the addition of ascorbate, methylene blue or SOD attenuated the increase in P-glycoprotein mRNA levels by SNP ($p<0.001$) (Fig. 6B).

Potential Involvement of NF-κB in the SNP-mediated Enhanced Expression of P-glycoprotein in MBEC4 Cells

To study the underlying mechanism for the SNP-mediated induction in the expression and the function of P-glycoprotein, we hypothesized that the exposure of an MBEC4 cell with the NO_x donor may lead to an activation of NF-κB, a putative regulator for P-glycoprotein expression (Thevenod et al., 2000; Kuo et al., 2002), thereby elevating the level of the P-glycoprotein expression and, thus, its function. Since NF-κB activation is involved in the translocation of the protein to the nucleus, the protein level was quantified in the nuclear fraction by Western blot analysis. Based on the gel electrophoresis data (Fig. 7A) and the software analysis of the band density, the nuclear translocation of NF-κB was readily apparent after 1 hr of the SNP treatment in MBEC4 cells, and the activation was still apparent up to 6 hr (i.e., the last sampling time) after SNP treatment (e.g., at 3 hr of SNP treatment, 155 ± 12.4 % of the band density of the untreated MBEC4 cells). In the case of the reference protein (i.e., β-actin), the density of the band was not affected by the SNP treatment. In addition, pretreatment with ascorbate (i.e., an antioxidant, 10 mM), methylene blue (i.e., an NO scavenger, 1mM) or

SOD (i.e., superoxide scavenger, 750 U/ml) attenuated nuclear translocation of NF-κB in MBEC4 cells exposed to SNP (1 mM, at 3 hr of treatment) (Fig.7B). To test this hypothesis further, electrophoretic mobility shift for NF-κB DNA binding activity was performed with the nuclear extracts of MBEC4 cells exposed to SNP using a radiolabeled NF-κB consensus oligonucleotide. SNP (1 mM, after 3 hr of treatment) markedly increased the binding activity of nuclear extracts to the NF-κB consensus oligonucleotide (Fig. 8A). The addition of 20-fold excess unlabeled NF-κB abolished the NF-κB DNA binding complex. Also, anti-p65 antibody supershifted the retarded band (Fig. 8B).

DISCUSSION

A diabetic condition induced by STZ is one of the most frequently used models of experimental diabetes. It is now well established that poorly controlled diabetes mellitus has a variety of adverse effects on the brain. Lass and Knudsen (1990) demonstrated that the resting cerebral blood flow values were reduced by 40% compared with the control value, suggesting that the physiological alteration may be related to the alteration in the transport of CsA across the BBB. However, since $CL_{app,br}$ of CsA was found to be 6.90 μl/min/g brain in diabetic rats, the value is much lower than the cerebral blood flow rate of the rat (i.e., 920 μl/min/g brain) (Kusuhara et al., 1997), suggesting the change in the blood flow to the brain is not likely to be the primary factor in the CsA transport. In addition, an *in vitro* observation of MBEC4 cells was consistent with the *in vivo* results. Furthermore, the brain uptake kinetics for mannitol, an impermeable substance to the BBB, was not affected by the induction of the diabetic condition, suggesting that the physical integrity of the barrier is not altered by the experimental diabetic condition.

In this study, mRNA levels of rMDR1a (4.01-fold), rMDR1b (2.91-fold) and rMRP2 (2.28-fold) were significantly elevated in STZ-induced diabetic rats compared with the control (Fig. 2) when normalized to mRNA level for β-actin (i.e., a reference marker). Consistent with the enhanced level of rMRP2 in diabetic rats, it was recently demonstrated that the permeability

of the BBB for fluorescein, a substrate for MRP2, was decreased in STZ-induced diabetic rats (Hawkins et al., 2007). Interestingly, however, rMRP1 mRNA levels were apparently unaffected in the diabetic condition, suggesting that certain specificity exists for the regulation of transporters in the BBB. In the case of rMDR1, the increase of protein level (1.92 fold) was somewhat comparable to that of the mRNA (2.91-4.01 fold).

In our study, we measured mRNA and protein levels of P-glycoprotein in whole brain homogenates rather than in brain microvessel endothelial cells in control and STZ-induced diabetic rats. The literature suggests that brain microvessel endothelial cells (viz, the BBB), not astrocytes and neurons, accounts for the majority of P-glycoprotein found in the brain tissue (Löscher and Potschka, 2005). In addition, higher P-glycoprotein expression was associated with higher function of the transporter in the BBB compared with the transporter in astrocytes (Declèves et al., 2000). Therefore, despite possible expression of P-glycoprotein in astrocytes and neurons and/or enhanced expression of the transporter in these cells under pathophysiological condition(s) (e.g., epilepsy) (Volk et al., 2004), the transporter in astrocytes and neurons may play a secondary role in the transport of CsA from the systemic circulation to the brain tissue. The function of P-glycoprotein in multiple brain cells warrants further investigation.

Since NO, a radical, is relatively reactive, the oxide form may produce a number of

DMD Fast Forward. Published on July 30, 2007 as DOI: 10.1124/dmd.107.015800
This article has not been copyedited and formatted. The final version may differ from this version.

NO_x (e.g., inorganic nitrite and peroxynitrite), depending on the rate of NO release. In the literature, SIN-1 and SNP were reported to produce predominantly peroxynitrite (viz, slow NO-releasing donors) while SNAP and DETA may preferentially generate NO and other nitrogen oxide (viz, rapid NO-releasing donors) (Walia et al., 2003). The results of this study indicate that the exposure of MBEC4 cells with slow NO-releasing donors led to a functional induction of P-glycoprotein while no effect on the function was noted for the case of the pretreatment of MBEC4 cells with rapid NO-releasing donors. Consistent with this observation, the stimulatory effect of SNP on the function and expression of P-glycoprotein was partially reversed by the presence of ascorbate (i.e., anti-oxidant), methylene blue (i.e., NO scavenger) or SOD (i.e., superoxide scavenger) (Fig 6). Taken together, these observations indicate that peroxynitrite, rather than NO itself or other nitrogen oxide forms, is involved in the functional induction of the efflux transporter. Since an increased formation of 3-nitrotyrosine (i.e., a by-product of the reaction between peroxynitrite and tyrosine residue of target protein) of proteins was found in the heart of mice with experimental diabetes (Cai et al., 2005), peroxynitrite may be endogenously over-produced in experimental diabetes. Consistent with the literature, we found that NO_x concentration was 117 ± 12.3 μM in the plasma of the diabetic rats. Therefore, the functional induction found in the present *in vivo* study may also be mediated by the overproduction of peroxynitrite. In addition, since NO_x level *in vivo* was comparable to that

measured in the *in vitro* culture condition (Table 3), the *in vitro* experimental condition appears relevant to the *in vivo* condition in terms of NO_x exposure.

In this study, it was suggested that the functional induction via the increased level of mRNA and protein for P-glycoprotein was mediated by the presence of SNP that potentially produce peroxynitrite *in vitro* (Fig. 5). In the literature, various factors that are involved in the transcription process are activated under nitrosative conditions. Among these, NF-κB is reported to be activated by peroxynitrite in various cell types. For example, the exposure to peroxynitrite donor SIN-1 increased a NF-κB-dependent luciferase reporter vector in rat lung epithelial cells (Janssen-Heininger et al., 1999), as well as iNOS protein levels via the activation of NF-κB in the bovine microvessel endothelium (Cook and Davidge, 2002). Consistent with the literature, the data from the present study indicate that the exposure of SNP to MBEC4 cells, an *in vitro* model of the BBB, leads to nuclear translocation of NF-κB (Fig.7) and increased DNA binding activity of nuclear extracts to the NF-κB consensus oligonucleotide (Fig. 8). It is believed that this represents the first indication in the literature wherein NF-κB activation has been observed in mice brain microvessel endothelial cells via SNP exposure. Our data collectively suggest NO_x (e.g., peroxynitrite) alters DNA binding activity of NF-κB, which, in turn, may enhance transcription of the P-glycoprotein, thereby inducing the expression and function of P-glycoprotein. Consistent with this hypothesis, a number of reports indicate that NF-κB is

involved in the increased gene expression for P-glycoprotein (Thevenod et al., 2000; Kuo et al., 2002), probably by a binding of NF-κB in the promoter region (Kuo et al., 2002).

Recently, Liu et al. (2006) reported that the induction of experimental diabetes led to an impaired function and expression of P-glycoprotein in the rat BBB, a result that directly contradicts the data obtained in the current study. The underlying reasons for the discrepancy are unknown. However, differences in the experimental design (e.g., difference in the STZ dosage, duration of diabetes, P-glycoprotein substrate used and/or the time of brain/blood sampling) may have contributed to the discrepancy. In addition, it is possible that the nitrosative stress may have a complex impact on P-glycoprotein function during the time-course of the stress progression, thus leading to contradictory results. For example, we demonstrated that *in vitro* nitrosative stress induced by SNP exposure led first to a transient impairment and, then, eventually to the induction of the transporter (Fig. 4C). Consistent with this observation, Bauer et al. (2007) recently reported that exposure of rat brain capillaries to TNF-α, an inflammatory mediator, caused a rapid decrease in P-glycoprotein transport activity in short-term (after 2-3 hr) and then a rapid increase in both function and expression via NF-κB activation in long-term (i.e., after 6 hr). Furthermore, the complex nature of nitrosative stress was documented in the regulation of the expression of transporters. For example, in another nitrosative model using lipopolysaccharide (LPS) treatment, function and/or expression of ABC transporters (i.e., P-

glycoprotein) were differentially regulated in a tissue-specific manner. Namely, LPS-induced acute inflammation caused down-regulation of P-glycoprotein in the liver, the intestine, and the brain, but up-regulation of P-glycoprotein in the kidney (Kalitsky-Szirtes et al., 2004; Hartmann et al., 2005; Wang et al., 2005; Heemskerk et al., 2007).

In this study, we investigated the role of nitrosative stress and alterations in the function/expression for P-glycoprotein both *in vivo* and *in vitro*. Zhou and Kuo (1997) found that addition of insulin independently induced the MDR1 gene in rat hepatocytes without nitrosative stress. Therefore, administration of insulin may induce function and expression of P-glycoprotein independent of nitrosative stress.

In conclusion, the induction of experimental diabetes led to a decrease in $CL_{app,br}$ for CsA, a well-known substrate for P-glycoprotein, which was associated with an increased level of mRNA and protein for the transporter. The induction in the function and the expression of P-glycoprotein was also noted in MBEC4 cells exposed to certain NO_x donors (e.g., SNP). The nuclear translocation of NF-κB and the increased DNA binding activity of nuclear extracts to the NF-κB consensus sequence were detected in MBEC4 cells pretreated with SNP. Since a variety of substrates are subjected to the efflux process via P-glycoprotein, the regulation may have a broad implication in understanding the altered pharmacokinetics of the substrates in experimental as well as clinical diabetes. Therefore, the regulatory mechanism for the efflux

transporter may be clinically relevant.

REFERENCES

Ahn SH, Jeon SH, Tsuruo T, Shim CK and Chung SJ (2004) Pharmacokinetic characterization of dehydroevodiamine in the rat brain. *J Pharm Sci* 93:283-292.

Bank N and Aynedjian HS (1993) Role of EDRF (nitric oxide) in diabetic renal hyperfilitration. *Kidney Int* 43:1306-1312.

Bauer B, Hartz AM and Miller DS (2007) Tumor necrosis factor alpha and endothelin-1 increase P-glycoprotein expression and transport activity at the blood-brain barrier. *Mol Pharmacol* 71:667-675.

Bridges CC, Shamsul ola M, Prasad PD, El-sherbeny A, Ganapathy V and Smith SB (2001) Regulation of taurine transporter expression by NO in cultured human retinal pigment epithelial cells. *Am J Physiol Cell Physiol* 281:C1825-C1836.

Cai L, Wang J, Li Y, Sun X, Wang L, Zhou Z and Kang YJ (2005) Inhibition of superoxide generation and associated nitrosative damage is involved in metallothionein prevention of diabetic cardiomyopathy. *Diabetes* 54:1829-1837.

Cooke CM and Davidge ST (2002) Peroxynitrite increases iNOS through NF-kB and decreases prostacyclin synthase in endotherial cells. *Am J Physiol Cell Physiol* 282:395-402.

Declèves X, Regina A, Laplanche JL, Roux F, Boval B, Launay JM and Scherrmann JM (2000) Functional expression of P-glycoprotein and multidrug resistance-associated protein (Mrp1) in

primary cultures of rat astrocytes. *J Neurosci Res* 60:594-601.

Green LC, Wagner DA, Glogowski J, Skipper PL, Wishnok JS and Tannenbaum SR (1982) Analysis of nitrate, nitrite, and [^{15}N] nitrate in biological fluids. *Anal Biochem* 126:131-138.

Hartmann G, Vassileva V and Piquette-Miller M (2005). Impact of endotoxin-induced changes in P-glycoprotein expression on disposition of doxorubicin in mice. *Drug Metab Dispos* 33:820-828.

Hawkins BT, Ocheltree SM, Norwood KM and Egleton RD (2007) Decreased blood-brain barrier permeability to fluorescein in streptozotocin-treated rats. *Leurosci Lett* 411: 1-5.

Heemskerk S, van Koppen A, van den Broek L, Poelen GJM, Wouterse AC, Dijkman HBPM, Russel FGM and Masereeuw R (2007) Nitric oxide differentially regulates renal ATP-binding cassette transporters during endotoxemia. *Pflugers Arch, in press.*

Huie RE and Padmaja S (1993) The reaction of NO with superoxide. *Free Radic Res Commun* 18:195-199.

Janssen-Heininger YMW, Macara I and Mossman BT (1999) Cooperativity between oxidants and tumor necrosis factor in the activation of (NF)-kB: requirement of Ras/mitogen-activated protein kinases in the activation of NF-kB by oxidants. *Am J Respir Cell Mol Biol* 20:942-952.

Kalitsky-Szirtes J, Shayeganpour A, Brocks DR, Piquette-Miller M (2004) Suppression of drug-metabolizing enzymes and efflux transporters in the intestine of endotoxin-treated rats. *Drug Metab Dispos* 32:20-27.

Krolewski AS, Warram JH and Rand LI (1987) Epidemiologic approach to the etiology of type I diabetes mellitus and its complications. *N Engl J Med* 317:1390-1398.

Kuo MT, Liu Z, Wei Y, Lin-Lee Y, Tatebe S, Mills GB and Unate H (2002) Induction of human MDR1 gene expression by 2-acetylaminofluorene is mediated by effectors of the phosphoinositide 3-kinase pathway that activate NF-kB signaling. *Oncogene* 21: 1945-1954.

Kusuhara H, Suzuki H, Terasaki T, Kakee A, Lemaire M and Sugiyama Y (1997) P-glycoprotein mediate the efflux of quinidine across the blood-brain barrier. *J Pharmacol Exp Ther* 283:574-580.

Lass P and Knudsen GM (1990) Cerebral blood flow response to propranolol in streptozotocin diabetic rats. *Neuroreport* 1:232-234.

Liu H, Xu X, Yang Z, Deng Y, Liu X and Xie L (2006) Impaired function and expression of P-glycoprotein in blood-brain barrier of streptozotocin-induced diabetic rats. *Brain Res* 1123:245-252.

Löscher W and Potschka H (2005) Blood-brain barrier active efflux transporters: ATP-binding cassette gene family. *NeuroRx* 2:86-98.

Lowry OH, Roseborough NJ, Farr AL and Randall RJ (1951) Protein measurement with the folin phenol reagent. *J Biol Chem* 193:265-275.

Matsuzaki J, Yamamoto C, Miyama T, Takanaga H, Matsuo H, Ishizuka H, Kawahara Y, Kuwano M, Naito M, Tsuruo T and Sawada Y (1999) Contribution of P-glycoprotein to bunitrolol efflux across blood-brain barrier. *Biopharm Drug Dispos* 20:85-90.

Mei Q, Richards K, Strong-Basalyga K, Fauty SE, Taylor A, Yamazaki M, Prueksaritanont T, Lin JH and Hochman J (2004) Using real-time quantitative TagMan RT-PCR to evaluate the role of dexamethasone in gene regulation of rat P-glycoproteins mdr1a/mdr1b and cytochrome P450 3A1/2. *J Pharm Sci* 93:2488-2496.

Obrosova IG, Mabley JG, Zsengellér Z, Charniauskaya T, Abatan OI, Groves JT and Szabó C (2005) Role for nitrosative stress in diabetic neuropathy: evidence from studies with a peroxynitrite decomposition catalyst. *FASEB J* 19:401-403.

Ogata M, Iizuka Y, Murata R and Hikichi N (1996) Effect of streptozotocin-induced diabetes on cyclosporin A disposition in rats. *Biol Pharm Bull* 19:1586-1590.

Pacher P, Obrosova IG, Mabley JG and Szabo C (2005) Role of nitrsative stress and peroxynitrite in the pathogenesis of diabetic complications. Emerging new therapeutical strategies. *Curr Medi Chem* 12:267-275.

Rodriguez BL, Curb JD, Burchfiel CM, Huang B, Sharp DS, Lu GY, Fujimoto W and Yano K (1996) Impaired glucose tolerance, diabetes, and cardiovascular disease risk factor profiles in the elderly: the honolulu heart program. *Diabetes Care* 19:587-590.

Schreiber E, Harshman K, Kemler I, Malipiero U, Schaffner W and Fontana A (1990) Astrocytes and glioblastoma cells express novel octamer-DNA binding proteins distinct from the ubiquitous Oct-1 and B cell type Oct-2 proteins. *Nucleic Acids Res* 18:5495-5503.

Serrano MA, Macias RIR, Vallezo M, Briz O, Bravo A, Pascual MJ, St-Pierre MV, Stieger B, Meier PJ and Marin JJG (2003) Effect of ursodeoxycholic acid on the impairment induced by maternal cholestasis in the rat placenta-maternal liver tandem excretory pathway. *J Pharmacol Exp Ther* 305: 515-524.

SZkudelski T (2001) The mechanism of alloxan and streptozotocin action in β cells of the rat pancreas. *Physiol Res* 50:536-546.

Takeuchi T, Yoshitomi S, Higuchi T, Ikemoto K, Niwa S, Ebihara T, Katoh M, Yokoi T and Asahi S (2006) Establishment and characterization of the transformants stably-expressing MDR1 derived from various animal species in LLC-PK1. *Pharm Res* 23:1460-1472.

Tatsuta T, Naito M, Oh-hara T, Sugawara I and Tsuruo T (1992) Functional involvement of P-glycoprotein in blood-brain barrier. *J Biol Chem* 267:20383-20391.

Thevenod F, Friedmann JM, Katsen AD and Hauser IA (2000) Up-regulation of multidrug resistance P-glycoprotein via nuclear factor-kappaB activation protects kidney proximal tubule cells from cadmium- and reactive oxygen species-induced apoptosis. *J Biol Chem* 275: 1887-1896.

Uchiyama T, Matsuda Y, Wada M, Takahashi S and Fujita T (2005) Functional regulation of Na+-dependent neutral amino acid transporter ASCT2 by S-nitrosothiols and nitric oxide in Caco-2 cells. *FEBS Lett* 579:2499-2506.

Van Waarde WM, Verkade HJ, Wolters H, Havinga R, Baller J, Bloks V, Muller M, Sauer PJJ and Kuipers F (2002) Differential effects of streptozotocin-induced diabetes on expression of hepatic ABC-transporters in rats. *Gastroenterology* 122:1842-1852.

Vliet EV, Aronica E, Redeker S, MArchi N, Rizzi M, Vezzani A and Gorter J (2004) Selective and persistent upregulation of mdr1b mRNA and P-glycoprotein in the parahippocampal cortex of chronic epileptic rats. *Epilepsy Res* 60:203-213.

Volk HA, Burkhardt K, Potschka H, Chen J, Becker A and Löscher W (2004) Neuronal expression of the drug efflux transporter P-glycoprotein in the rat hippocampus after limbic seizures. *Neuroscience* 123:751-759.

Walia M, Samson SE, Schmidt T, Best K, Whittington M, Kwan CY and Grover AK (2003) Peroxynitrite and nitric oxide differ in their effects on pig coronary artery smooth muscle. *Am J Physiol Cell Physiol* 284:C649-C657.

Wang JH, Scollard DA, Teng S, Reilly RM and Piquette-Miller M (2005) Detection of P-glycoprotein activity in endotoxemic rats by 99mTc-sestamibi imaging. J Nucl Med 46:1537-1545.

Zhou G and Kuo MT (1997) NF-kappaB-mediated induction of mdr1b expression by insulin in rat hepatoma cells. *J Biol Chem* 272:15174-15183.

FOOTNOTES

This study was supported by a grant (A03-0001-A71005-06M4-13010A) from Ministry of Health & Welfare, Republic of Korea, and a grant from the health fellowship foundation.

Suk-Jae Chung, Ph.D.

Department of Pharmaceutics, College of Pharmacy, Seoul National University

San 56-1, Shinlim-dong, Kwanak-gu, Seoul 151-742, Korea

Figure legends

Fig. 1. Temporal dependency on P-glycoprotein function for STZ-induced diabetic rats during the treatment period. The brain uptake clearance of CsA was estimated by standard integration plot analysis as described under *Materials and Methods.* ***$p < 0.001$, from the control group by unpaired Student's *t* test. The data are expressed as mean ± SD of 3-5 rats.

Fig. 2. Gene expression of MDR1a, MDR1b, MRP1 and MRP2 by quantitative RT-PCR analysis in control and STZ-induced diabetic rats. Levels of ABC transporter mRNAs were determined by the quantitative RT-PCR as described under *Materials and Methods.* Data shown correspond to transporter mRNA levels are expressed in the fold change of those found in control rats. *$p < 0.05$, **$p < 0.01$ from the control group by unpaired Student's *t* test. The data are expressed as mean ± SD of 3 rats.

Fig. 3. Protein expression of P-glycoprotein in the brain of control and STZ-induced diabetic rats. Panel A shows the immunoblot of brain homogenates from control or STZ-induced diabetic rats, probed with P-glycoprotein antibody. Panel B represents the normalized (i.e., with the band density for β-actin) density for P-glycoprotein band in the brain of control and STZ-induced diabetic rats. The data are expressed in % of the control value. Western blot analysis was performed to measure levels of P-glycoprotein of brain homogenate as described under *Materials and Methods.* Molecular mass of transporter is indicated on the right. ***$p < 0.001$

from the control group by unpaired Student's *t* test. The data in Panel B represent mean ± SD of 4 rats.

Fig. 4. Comparison of the function of P-glycoprotein in MBEC4 Cells in the presence of various NO_x donors. Panel A represents the 15 min uptake of [^{3}H] CsA (1 μM) in the absence or presence of 1 mM S-nitroso-N-acetyl-DL-penicillamine (SNAP), diethylenetriamine (DETA), 3-morpholinosydnonimine (SIN-1), sodium nitroprusside (SNP) for 24 hr. Confluent cells were incubated with various NO_x donors (1 mM), and then CsA uptake in MBEC4 cells was measured as described under *Materials and Methods.* Panel B represents the dependency of SNP concentration (i.e., 24 hr exposure) on the uptake of [^{3}H] CsA (1 μM). Panel C represents the temporal profile of P-glycoprotein function by the pretreatment of SNP at 1 mM (n=4 mean ± SD). *$p < 0.05$, ***$p < 0.001$, from the control group by one-way ANOVA, followed by Duncan's test. The data are expressed as mean ± SD (n=4).

Fig. 5. The level of mRNA expression and protein expression for P-glycoprotein in MBEC4 cells with or without SNP exposure. Panel A shows electrophoretic separation of the amplification products obtained with a semiquantitative RT-PCR using specific primer sets for P-glycoprotein (Key: MDR1b) and glyceraldehyde-3-phosphate dehydrogenase (Key: GAPDH) in control and SNP treated (i.e., 1 mM, 24 hr exposure) MBEC4 cells as described under *Materials and Methods* section. Panel B represents mRNA expression of MDR1b by

quantitative RT-PCR analysis in control and SNP-pretreated (i.e., 1 mM, 24 hr exposure) MBEC4 cells. Level of MDR1b mRNA were determined by the quantitative RT-PCR as described under *Materials and Methods.* The data are expressed in the fold change of those found in control cells. The data in Panel B are expressed as mean ± SD of triplicate runs. ***$p <$ 0.001 from the control group by unpaired Student's *t* test. Panel C represents the immunoblot of cell lysates from control or SNP-pretreated (i.e., 1 mM, 24 hr exposure) MBEC4 cells, probed with P-glycoprotein antibody. Western blot analysis was performed to measure levels of P-glycoprotein of cell lysates as described under *Materials and Methods.* Molecular mass of transporter is indicated on the right. The results were confirmed by repeated experiments.

Fig. 6. Effect of the function and expression of P-glycoprotein in the presence of potential reversal agents for the NO_x stimulatory effect. Panel A represents the function of P-glycoprotein in the presence of ascrobate (10 mM, i.e., an antioxidant) or methylene blue (1 mM, i.e., a scavenger of NO) or SOD (750 U/ml) along with SNP exposure (i.e., 1 mM, 24 hr treatment) in MBEC4 cells. Confluent cells were incubated with SNP in the presence of various potential reversal agents and the uptake of CsA determined under *Materials and Methods.* Panel B represents the mRNA levels of P-glycoprotein in the presence of ascrobate (10 mM, i.e., an antioxidant), methylene blue (1 mM, i.e., a scavenger of NO) or SOD (750 U/ml) along with SNP exposure (i.e., 1 mM, 24 hr treatment) in MBEC4 cells. Level of MDR1b mRNA were

determined by the quantitative RT-PCR as described under *Materials and Methods.* The data are expressed in the fold change of those found in control cells. $^{**}p < 0.01$, $^{***}p < 0.001$, from the control group by one-way ANOVA, followed by Duncan's test. The data are expressed as mean ± SD (n=3~4).

Fig. 7. The level of NF-κB in the nucleus of MBEC4 cells with or without SNP exposure and the effects of ascrobate, methylene blue or SOD on NF-κB activation. Panel A represents the immunoblot of the nuclear lysate of MBEC4 cells with or without SNP exposure (1 mM), probed with NF-κB specific antibody as described under *Materials and Method* section. The time of SNP exposure was labeled in the photographic representation. Panel B represent the immunoblot of the nuclear lysates of MBEC4 pretreated with SNP (1 mM, for 3 hr) in the presence of ascorbate or methylene blue or SOD, probed with NF-κB specific antibody. The results were confirmed by repeated experiments.

Fig. 8. Gel shift analyses of NF-κB transcription complexes. Panel A represents gel shift assay performed using the nuclear extracts prepared from MBEC4 cells with or without SNP exposure (1 mM) for 1 ~ 6 hr. Each lane contained 30 μg of nuclear extracts and 5 ng of the labeled NF-κB consensus oligonucleotide. Panel B represent supershift of NF-κB bound with DNA. A competition study was carried out by adding a 20-fold excess of the unlabeled NF-κB-binding oligonucleotide or a 20-fold excess of the unlabeled SP-1-binding oligonucleotide. An antibody

competition experiment was conducted by incubating the nuclear extracts prepared from cells pretreated with 1mM SNP for 3 hr, with the specific antibody directed against the p65 protein. The *arrowhead(s)* indicate(s) the p65/p60 dimer bound with DNA (*closed arrowhead*) and the supershifted NF-κB DNA complex (*open arrowhead*). The results were confirmed by repeated experiments.

DMD Fast Forward. Published on July 30, 2007 as DOI: 10.1124/dmd.107.015800
This article has not been copyedited and formatted. The final version may differ from this version.

Table 1. Characteristics of control and STZ-induced diabetic rats (n=3~6, mean ± SD) 28 days after the treatment.

	Glucose level (mg/dl)	Body weight change (g)	NO_x (μM)
Control	71.5 ± 5.45	91.7 ± 2.89	35.9 ± 3.82
Diabetes	500 ± 23.7***	- 48.3 ± 18.9***	117 ± 12.3***

[a] ***$p < 0.001$ from the control group by unpaired Student's *t* test. The data are expressed as mean ± SD of 3~6 rats.

DMD Fast Forward. Published on July 30, 2007 as DOI: 10.1124/dmd.107.015800
This article has not been copyedited and formatted. The final version may differ from this version.

Table 2. Brain distribution of [^{3}H] cyclosporin A after intravenous administration

	n	$K_{p,brain}$ *(μl/g brain)*	$CL_{app,br}$ *(μl/min/g brain)*
Control	4	56.9 ± 5.66	11.8 ± 0.947
Diabetes	5	37.5 ± 7.43***	6.90 ± 1.37***

[a] ***$p < 0.001$ from the control group by unpaired Student's *t* test. The data are expressed as mean ± SD of 4~5 rats.

DMD Fast Forward. Published on July 30, 2007 as DOI: 10.1124/dmd.107.015800
This article has not been copyedited and formatted. The final version may differ from this version.

Table 3. Nitric oxide form(s) generation in MBEC4 medium following incubation SNAP, DETA, SIN-1 or SNP for 24 hr

Treatment	*NO_x (μM)*
Medium only	21.1 ± 15.3
SNAP (1 mM)	355 ± 10.9***
DETA (1 mM)	977 ± 27.7***
SIN-1 (1 mM)	774 ± 27.7***
SNP (1 mM)	158 ± 20.0***

[a] ***$p < 0.001$ from the medium only group by one-way ANOVA, followed by Duncan's test. The data are expressed as mean ± SD of 4 independent experiments.

DMD Fast Forward. Published on July 30, 2007 as DOI: 10.1124/dmd.107.015800
This article has not been copyedited and formatted. The final version may differ from this version.

Fig. 1.

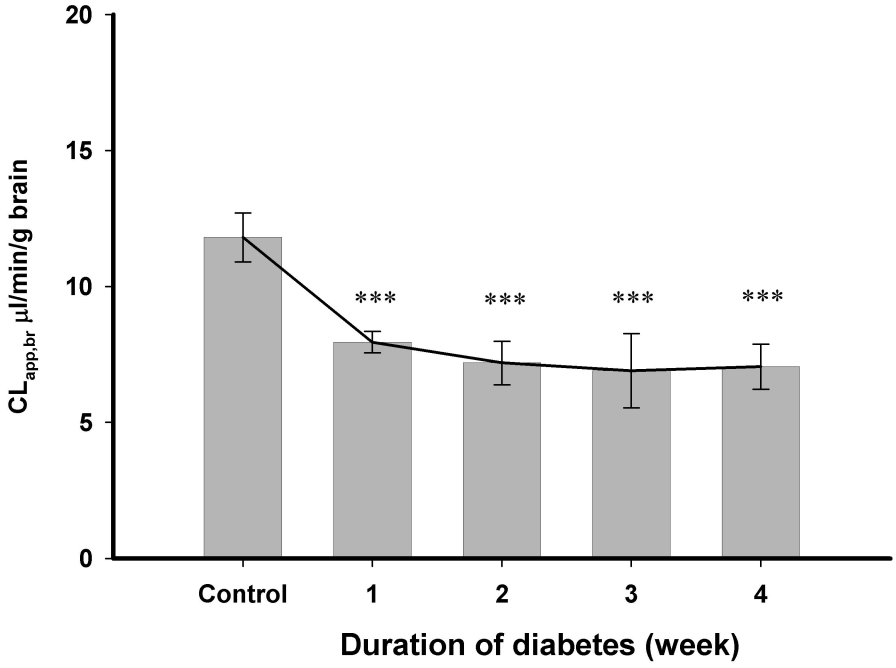

DMD Fast Forward. Published on July 30, 2007 as DOI: 10.1124/dmd.107.015800
This article has not been copyedited and formatted. The final version may differ from this version.

Fig. 2.

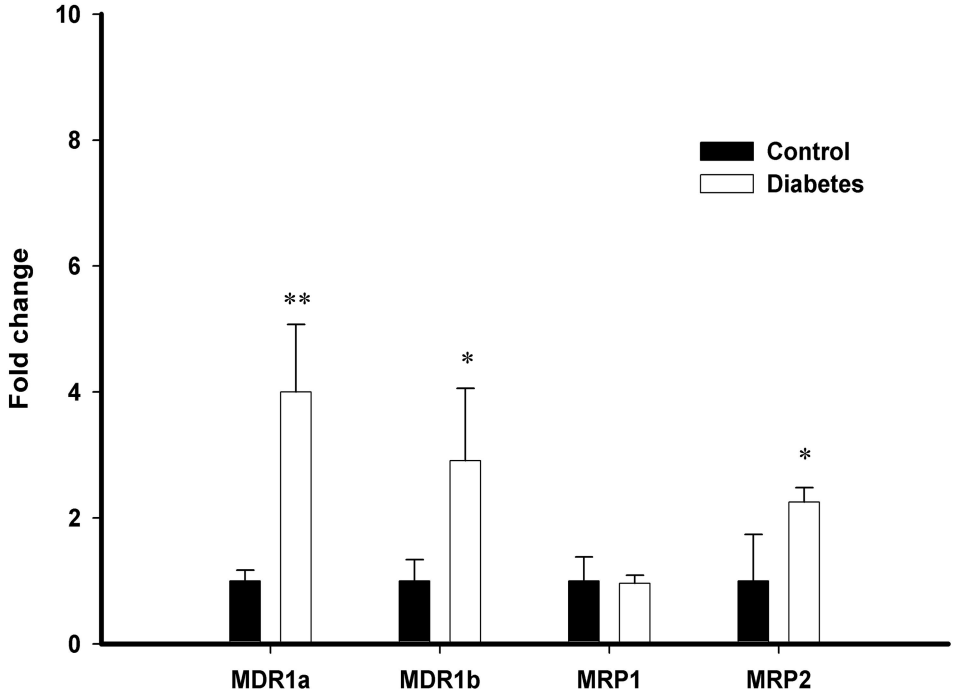

DMD Fast Forward. Published on July 30, 2007 as DOI: 10.1124/dmd.107.015800
This article has not been copyedited and formatted. The final version may differ from this version.

Fig. 3.

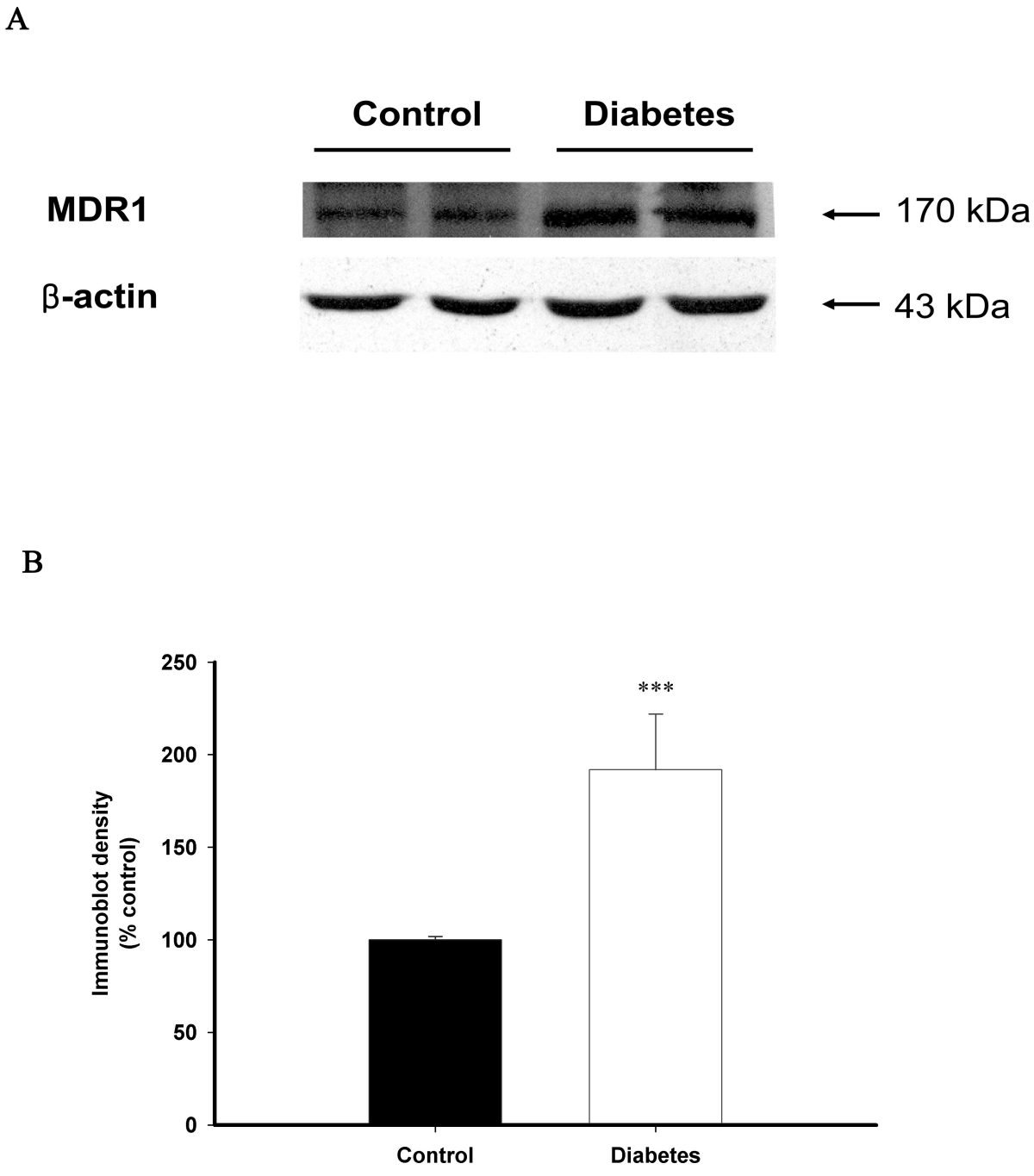

Fig. 4.

DMD Fast Forward. Published on July 30, 2007 as DOI: 10.1124/dmd.107.015800
This article has not been copyedited and formatted. The final version may differ from this version.

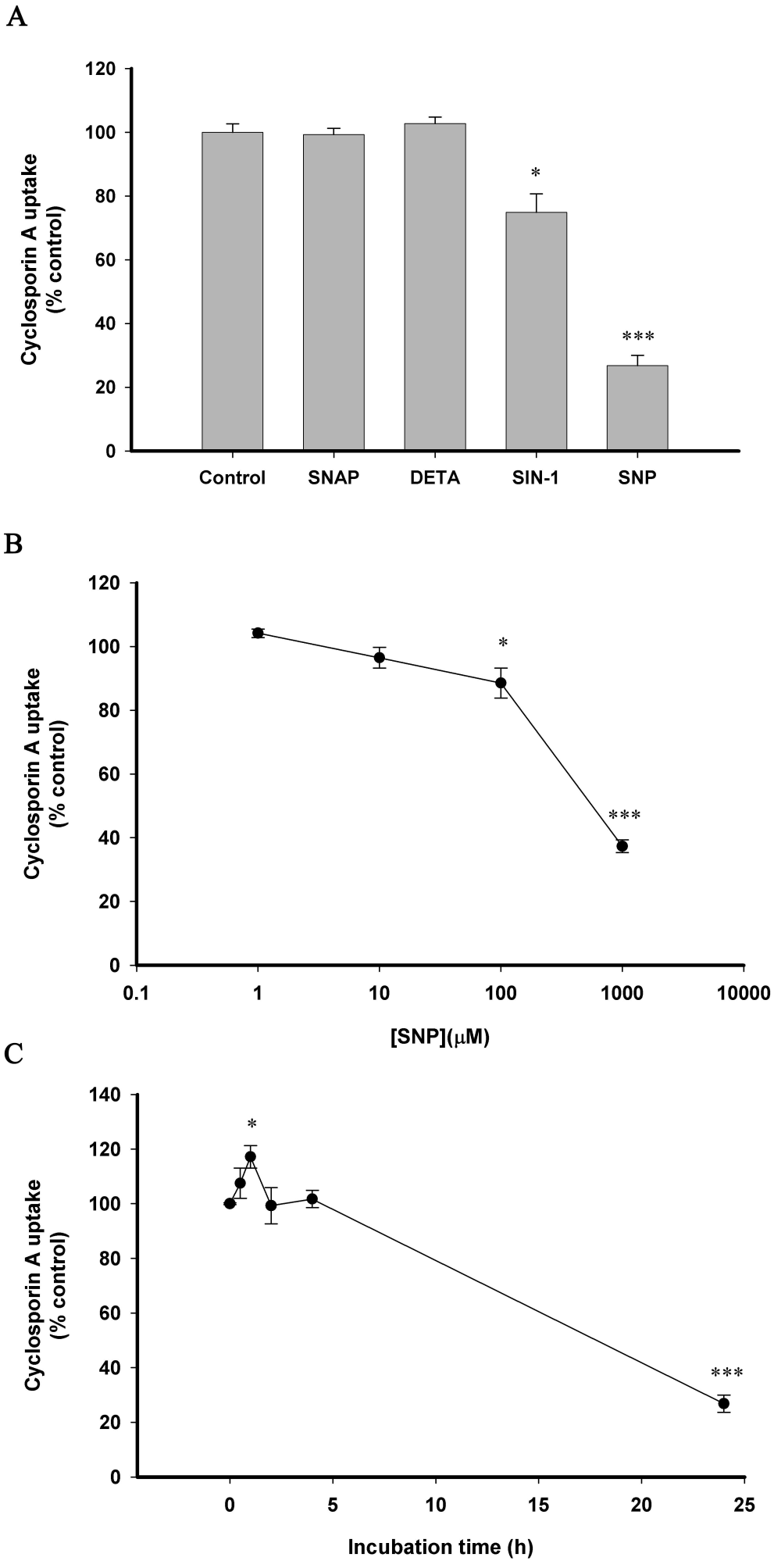

DMD Fast Forward. Published on July 30, 2007 as DOI: 10.1124/dmd.107.015800
This article has not been copyedited and formatted. The final version may differ from this version.

Fig. 5.

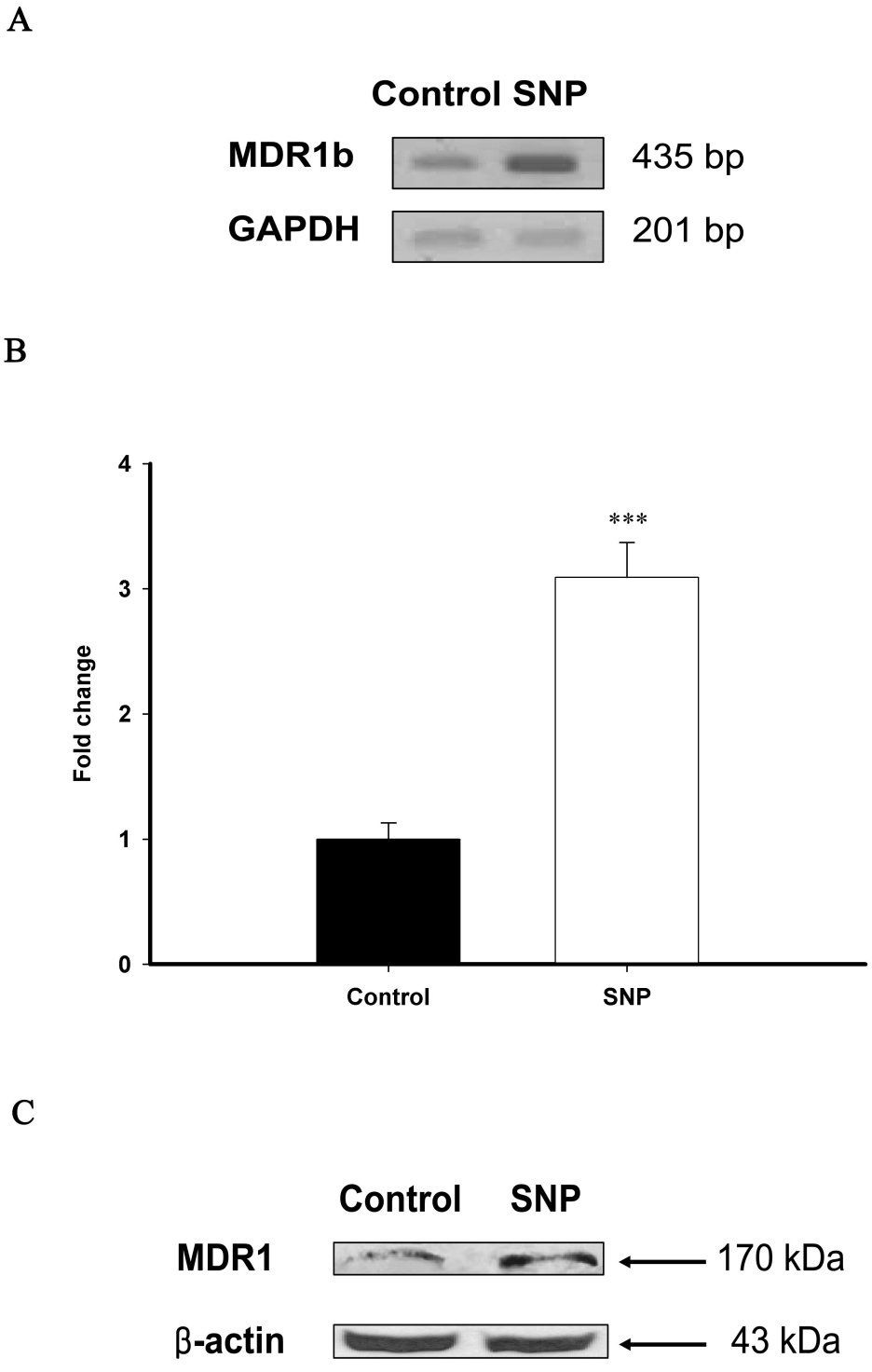

DMD Fast Forward. Published on July 30, 2007 as DOI: 10.1124/dmd.107.015800
This article has not been copyedited and formatted. The final version may differ from this version.

Fig. 6.

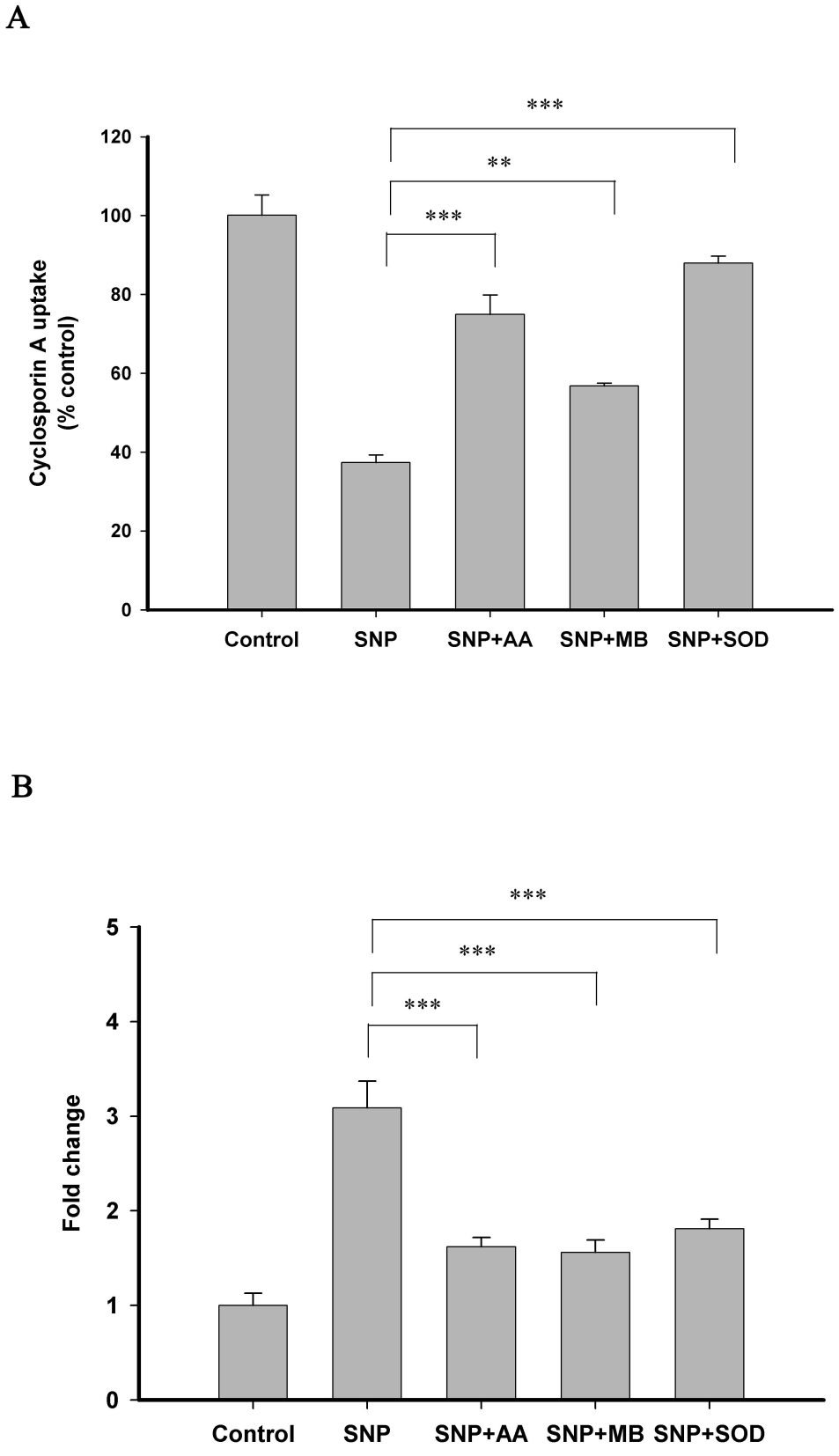

DMD Fast Forward. Published on July 30, 2007 as DOI: 10.1124/dmd.107.015800
This article has not been copyedited and formatted. The final version may differ from this version.

Fig. 7.

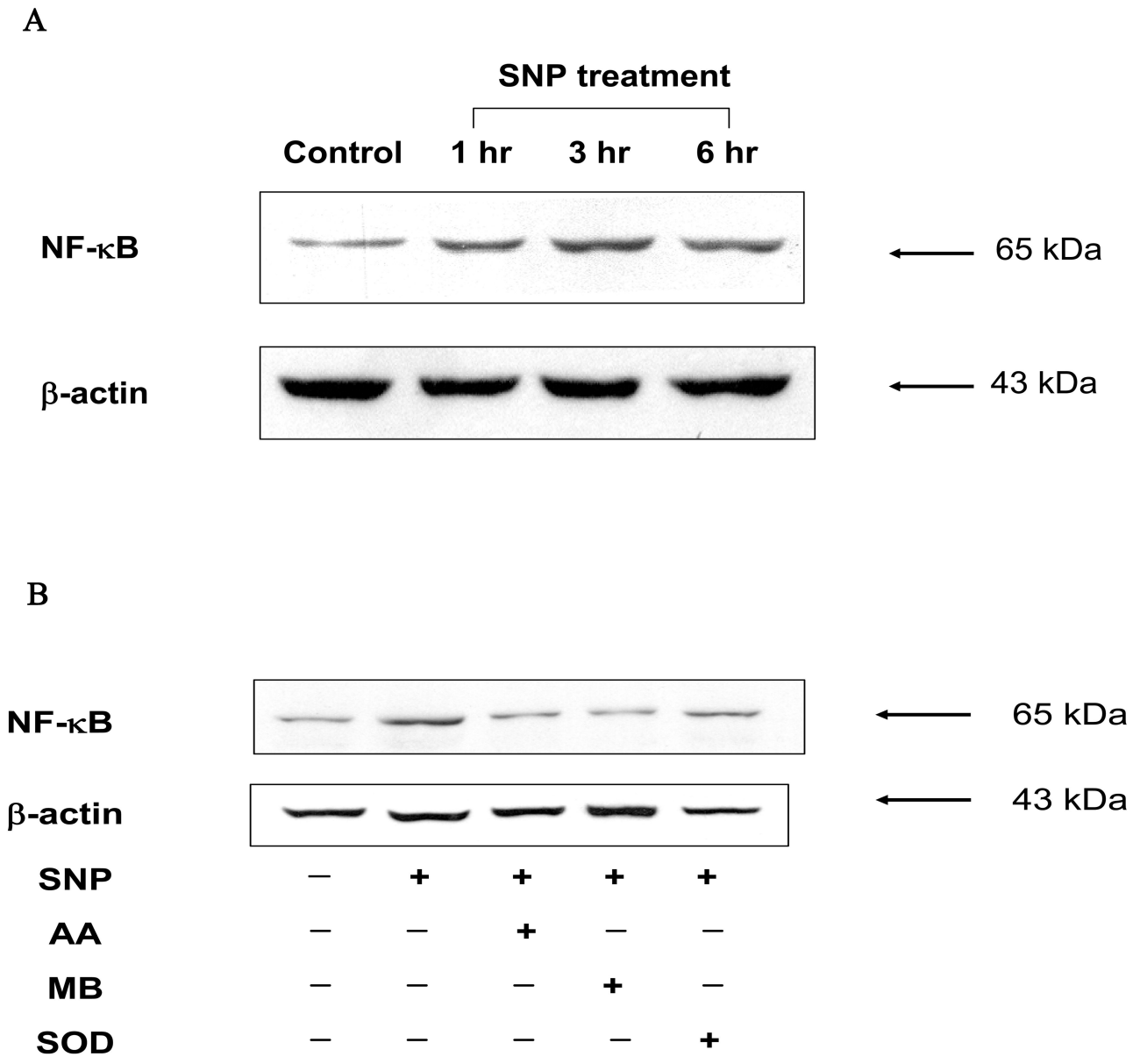

DMD Fast Forward. Published on July 30, 2007 as DOI: 10.1124/dmd.107.015800
This article has not been copyedited and formatted. The final version may differ from this version.

Fig. 8.